

INFLUENCE OF HIGH-SPEED TRAIN POWER CONSUMPTION ON A NOVEL GROUND FAULT IDENTIFICATION METHOD FOR 2×25 KV RAILWAY POWER SUPPLY SYSTEMS

J. SERRANO, C.A. PLATERO, M. LÓPEZ-TOLEDO & R. GRANIZO

Department of Electric Engineering, E.T.S.I. Industriales, Politecnical University of Madrid, Spain.

ABSTRACT

Nowadays, the most commonly used configuration to supply high-speed trains is 2×25 kV power supply system. The location of ground faults in 2×25 kV power supply systems is a difficult task, since the use of distance protection relays to localize ground faults positions doesn't work properly as the relation between the distance and the impedance seen by the distance protection relays is not linear and therefore the location is not accurate enough. A new simple and economical method to identify the subsection between autotransformers (ATS) and the conductor (positive or negative) where the ground fault is happening, based on the comparison of the angle between the current and the voltage of the positive terminal in each autotransformer, was developed recently. Consequently, after the identification of the subsection and the conductor with the ground fault, only this subsection where the ground fault is present, will be quickly removed from service, with the minimum effect on rail traffic. The high-speed trains demand a power about 12–16 MW, hence a significant current flow through the conductors of the 2×25 kV power system. This paper presents a study about the influence of the current consumed by the high-speed trains on this novel ground fault identification method. The operation of the method is correct even with the high-speed train currents in the section with a ground fault. This fact has been validated through numerous computer simulations, obtaining excellent results.

Keywords: fault location, ground faults, protection, 2×25 kV, railways.

1 INTRODUCTION

At present, the usual method of providing high levels of power to feed high-speed trains is a traction system called 2×25 kV. This power supply system has a positive conductor (usually called catenary) at 25 kV AC voltage with a positive polarity with respect to ground, and a negative voltage conductor (usually called feeder) at 25 kV AC voltage with a negative polarity with respect to ground. The supply to the trains employs the catenary and the grounded rail.

In these power systems, the complete traction line is supplied by several traction substations (TS). Each TS supplies two sections. Moreover, in each section, there are several subsections at regular intervals which are delimited by stations with power ATS. At the end of each section another autotransformer station (SATS) is installed. In Fig. 1 a traction line section with three subsections is shown, as well as the theoretical current distribution.

In 2×25 kV power systems, the traction power demanded is delivered at 50 kV while it is used at 25 kV. This fact reduces the current needed to supply the power required by high-speed trains [1]. In consequence, the length of the sections can be greater and the number of TS lower.



This paper is part of the proceedings of the 15th International Conference on Railway Engineering Design and Operation (COMPRAIL)

www.witconferences.com

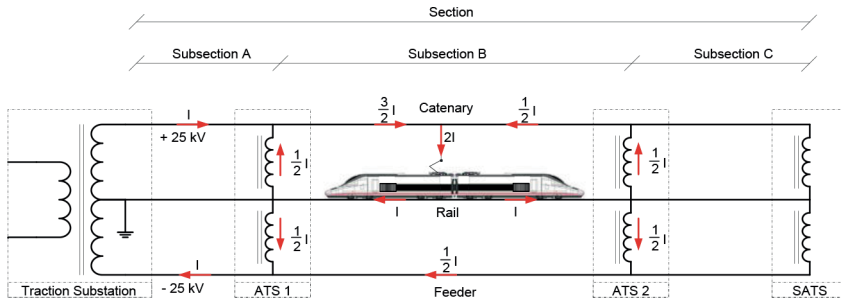


Figure 1: Simplified diagram of a 2×25 kV power system and currents distribution in a section comprising three subsections.

Another remarkable advantage of the 2×25 kV traction systems is the great reduction of electromagnetic interference on communication facilities and railway signalling circuits (signalling track circuits) as well as on nearby telecommunication lines [2, 3].

Railway traction systems have frequent external faults caused by accidental events. In the 2×25 kV power systems most of them are caused by outdoor short circuits between the catenary or the feeder to ground [4, 5]. But in this system, the ratio between the impedance (Z) seen from the TS and the distance to the ground fault is non-linear because of the use of ATS. This ratio is as shown in Fig. 2 [6, 7]. That is why it is so complex to use efficiently in the 2×25 kV lines the protection system based on distance protection relays [8].

This complexity of the detection and location of ground faults in the 2×25 kV lines means that the identification of the subsection and the conductor where the ground fault has happened [6, 9] is the main task of the protection systems in order to disconnect immediately the conductor with the ground fault in the corresponding subsection [10]. So only trains running in the subsection with the ground fault, in the case where the fault is in the catenary, will be disconnected from the power supply. Serrano et al. [11] describe a new method for identifying the subsection and the conductor (catenary or feeder) in which there is a ground fault in an easy and economical way. As the identification is done immediately, the subsection and conductor can be disconnected while keeping the rest of the power system in service. Besides, to implement this method, a small investment is required.

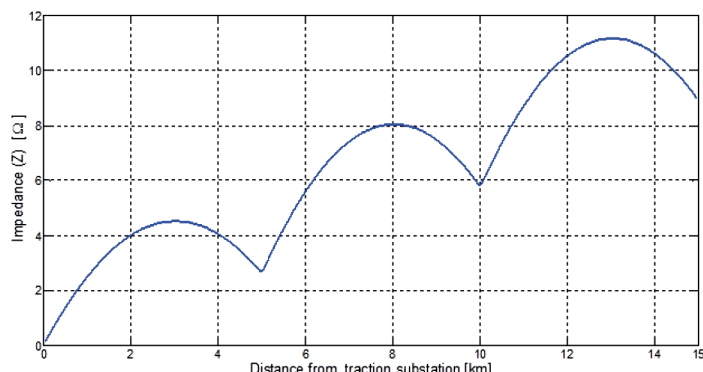


Figure 2: Modulus of the fault impedance seen from the traction substation in function of the distance in 2×25 kV traction power systems.

This paper presents a study about the influence of the current consumed by the high-speed trains on this novel ground fault identification method. In Section 2 an overview of this identification method is presented. In Section 3 the influence of high-speed train power consumption on this novel ground fault identification method is analysed. Finally, in Section 4 conclusions are shown.

2 GROUND FAULT IDENTIFICATION METHOD FOR 2×25 KV RAILWAY POWER SUPPLY SYSTEMS

2.1 Description of the method

In normal operation of 2×25 kV traction power supply system, the phase angle between voltage and current in the autotransformer is close to 180° (Fig. 3), according to the theoretical current distribution previously shown in Fig. 1 [11].

When there is a ground fault on a line between the catenary and rail or between the feeder and rail in a 2×25 kV traction power system, there is a substantial increase in the current circulating through the windings of the ATS closest to the defect location. This current increase can be detected easily by measuring the currents in the windings of the ATS. Furthermore, when the fault happens, the angles between the currents and voltages shift by 90° in the ATS closest to the fault location. In the case of a ground fault between the catenary and rail, the phase angle between the voltage and current in these ATS will result in 90° while in the case of ground fault between the feeder and rail, these angle will be 270° .

Figure 4 shows an example of a ground fault between catenary and rail in section B. In this particular case, the angles between I_{A1} and V_{C1} and between I_{A2} and V_{C2} , respectively, change their values from approximately 180° to 90° . Also, there is a great increase in the module of I_{A1} and I_{A2} .

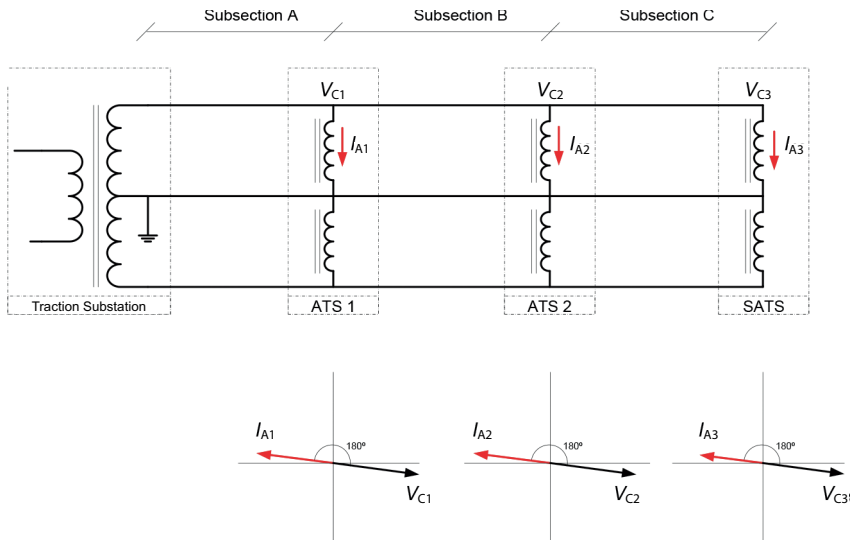


Figure 3: 2×25 kV power system currents (I_A) and voltages (V_C) distribution in normal operation.

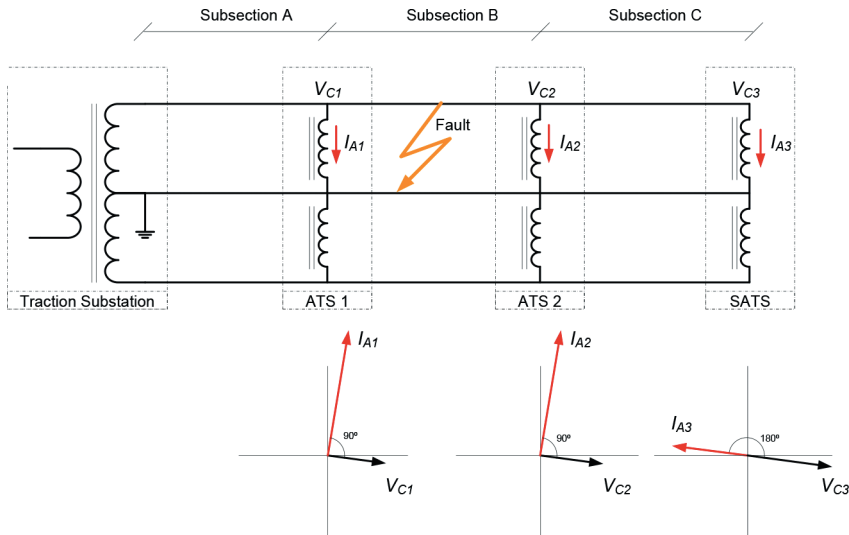


Figure 4: 2×25 kV power system currents (I_A) and voltages (V_C) distribution with a ground fault in the catenary in subsection B.

Another example can be seen in Fig. 5. It shows a ground fault between feeder and rail in section C. The current increase in this case will affect only currents I_{A2} and I_{A3} and there will be no remarkable change in current I_{A1} . The angles between I_{A2} and V_{C2} , and I_{A3} and V_{C3} , respectively, will change, but not the angle between I_{A1} and V_{C1} . These phase angle changes will be from 180° to 270° .

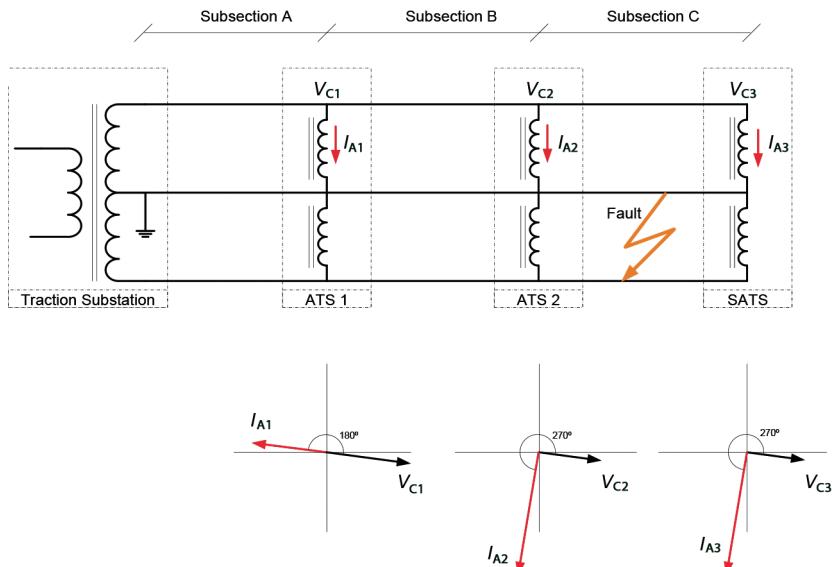


Figure 5: 2×25 kV power system currents (I_A) and voltages (V_C) distribution with a ground fault in the feeder in subsection C.

Table 1: Angle variation between I_A and V_C as a function of the subsection with the ground fault.

	ATS1	ATS2	ATS3
Fault at catenary in subsection 1	90°	180°	180°
Fault at feeder in subsection 1	270°	180°	180°
Fault at catenary in subsection 2	90°	90°	180°
Fault at feeder in subsection 2	270°	270°	180°
Fault at catenary in subsection 3	180°	90°	90°
Fault at feeder in subsection 3	180°	270°	270°

The changes of the angle between the currents and voltages when there is a ground fault in the system represented in Fig. 3 are listed in Table 1.

In this way, measuring the I_A module and the phase angle between V_C and I_A , it is possible to know the subsection and the conductor where the ground fault has happened.

2.2 Simulation model

In order to validate the new method [11] numerous computer simulations have been carried out using modified nodal circuit analysis method ran on MATLAB® software applied to the circuit shown in Fig. 6.

The experimental circuit is supplied from one end with two 25 kV AC sources with reverse polarity in each one. This circuit has three subsections A, B and C, each with a length of 10 km.

Self and mutual impedances values used in the simulations are listed in Table 2.

Table 2: Self and mutual impedances values of the railway conductors.

Conductor	Impedance[Ω/km]	Conductor	Impedance[Ω/km]		
Catenary	Z_C	$0.1197 + j0.6224$	Catenary–feeder	Z_{CF}	$0.0480 + j0.3401$
Feeder	Z_F	$0.1114 + j0.7389$	Catenary–rail	Z_{CR}	$0.0491 + j0.3222$
Rail	Z_R	$0.0637 + j0.5209$	Feeder–rail	Z_{FR}	$0.0488 + j0.2988$

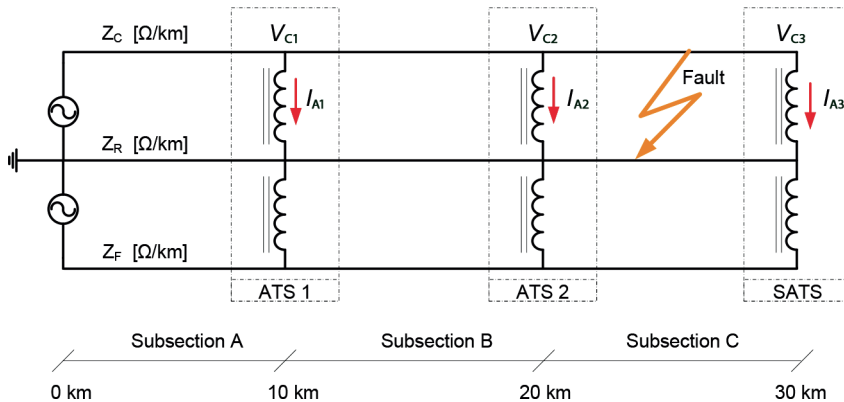


Figure 6: Simulated 2 × 25 kV power supply system.

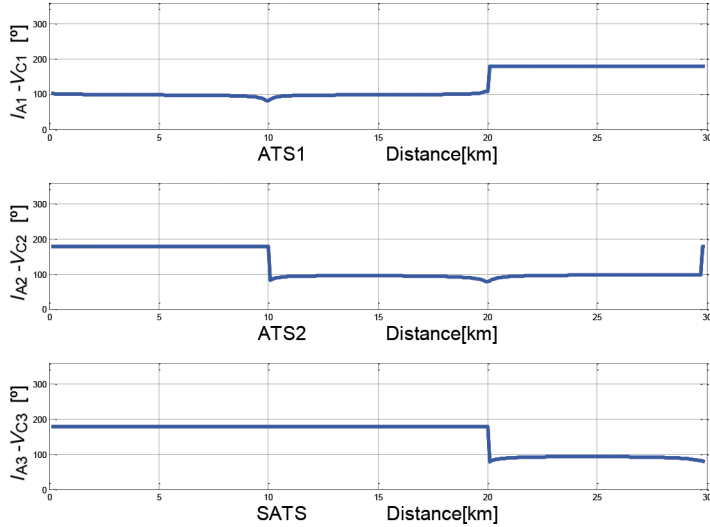


Figure 7: Phase angles between I_A and V_C at different ATS. Fault between catenary and rail.

Employing this circuit, different MATLAB® simulations were developed, performing short circuits between the catenary and rail, and between the feeder and rail. These short circuits were simulated at all the points along the three subsections A, B and C of the 30 km section. The phase angles between the currents $I_{A1}-I_{A2}-I_{A3}$ and the voltages $V_{C1}-V_{C2}-V_{C3}$ in the ATS ATS1, ATS2 and SATS, as a function of the distance from the TS where the fault has happened between the catenary and rail, are represented in Fig. 7. The axes used in Fig. 7 are scaled from 0 to 30 km and from 0° to 360° . It can be observed that if the fault happens in subsection A along the first 10 km, the angle between the current I_{A1} and voltage V_{C1} in the ATS1 is about 90° . However, such angles at ATS2 and SATS are 180° . Likewise, if the fault is in subsection B (between 10 and 20 km) the phase angles between the current I_{A1} and the voltage V_{C1} , and between the current I_{A2} and the voltage V_{C2} , will be about 90° at both ATS1 and ATS2, while at SATS this angle is close to 180° . It can also be seen that if the fault is in subsection C (between 20 and 30 km), the angle is about 90° at ATS2 and SATS but 180° at ATS1.

In the case where the fault happens between the feeder and rail, the results obtained are similar when the fault takes place between the catenary and rail, except that now the angles between the currents $I_{A1}-I_{A2}-I_{A3}$ and the voltages $V_{C1}-V_{C2}-V_{C3}$ are 270° instead of 90° . Figure 8 shows how the variations of these phase angles as a function of the distance to the fault from the substation follow the same pattern as in the case of a fault between the catenary and rail, but now with values close to 270° .

3 INFLUENCE OF HIGH-SPEED TRAIN POWER CONSUMPTION ON THIS NOVEL GROUND FAULT IDENTIFICATION METHOD

In order to study the influence of the train consumption in the operation of the new identification method, a current source has been added to the circuit previously shown in Fig. 6. The current I considered is 616 A with a 0.95 power factor, which represents a high-speed train consumption during the acceleration process. In this case, the current source is placed in the midpoint of the subsection B in Fig. 9, but different train locations have been studied.

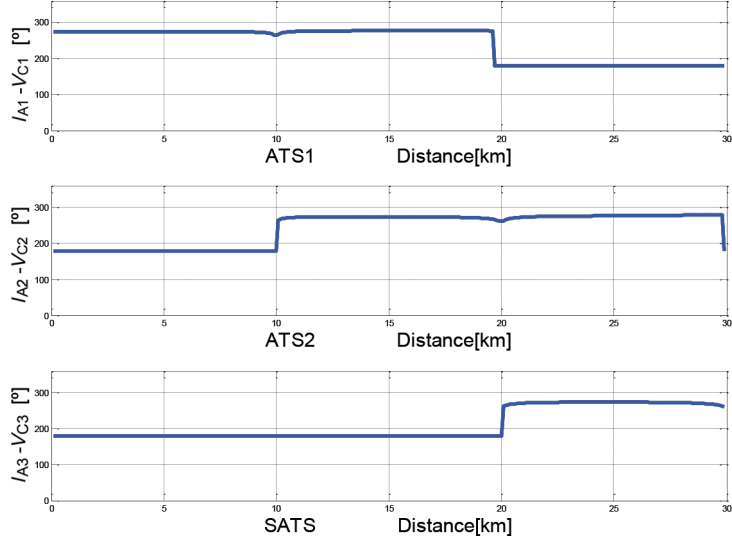


Figure 8: Phase angles between I_A and V_C at different ATS. Fault between feeder and rail.

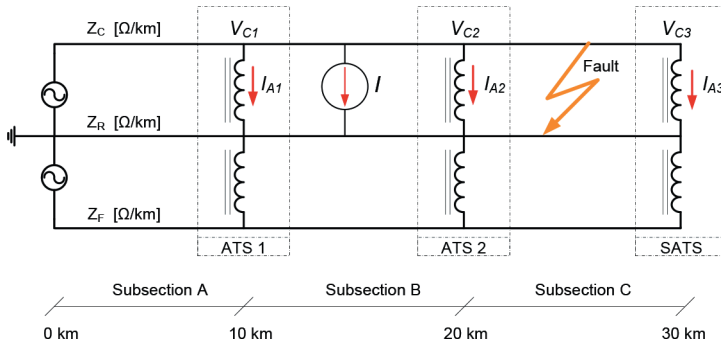


Figure 9: Simulated 2×25 kV power supply system including a train.

New MATLAB® simulations were developed on this modified circuit, performing short circuits between the catenary and rail, and between the feeder and rail. These short circuits were simulated at all points along the three subsections A, B and C of the 30 km section, including the presence of one or two trains in the middle of A, B and C subsections. In this way, the phase angles between the currents $I_{A1}-I_{A2}-I_{A3}$ and the voltages $V_{C1}-V_{C2}-V_{C3}$ in the ATS ATS1, ATS2 and SATS, as a function of the distance from the traction substation, are obtained when a ground fault has happened.

Among all the simulations performed, several results are presented in this section as example.

The phase angles in case of short circuit between catenary and rail are shown in Fig. 10, including a train in the midpoint of subsection B.

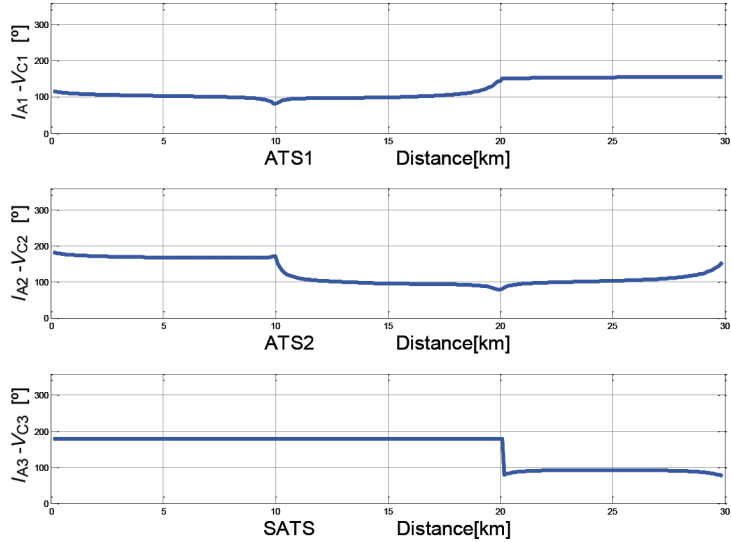


Figure 10: Phase angles between I_A and V_C at different ATS. Fault between catenary and rail. A train is simulated at the middle point of subsection B.

In case of short-circuit between feeder and rail, the results are represented in Fig. 11. In this case the train is placed at the midpoint of the subsection A.

The results in case of two trains in the same section are shown in Figs 12 and 13.

In Fig. 12 the short circuits considered are catenary–rail, and the trains are placed in the subsections A and B, respectively.

In Fig. 13 the case corresponds to short circuits between feeder and rail with two trains in the subsections A and C.

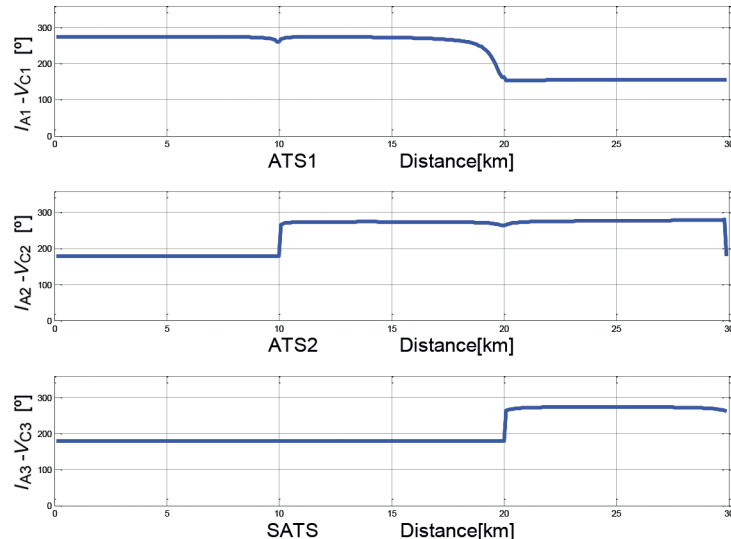


Figure 11: Phase angles between I_A and V_C at different ATS. Fault between feeder and rail. A train is simulated at the middle of subsection A.

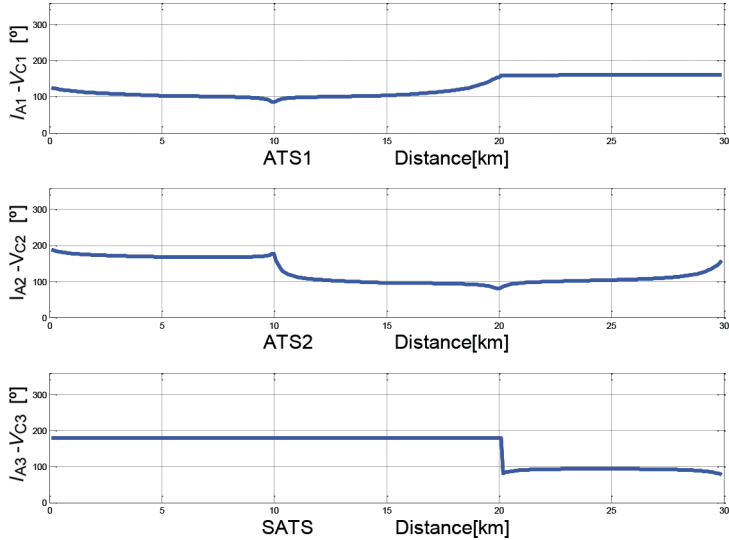


Figure 12: Phase angles between I_A and V_C at different ATS. Fault between catenary and rail. Two trains are placed at subsections A and B.

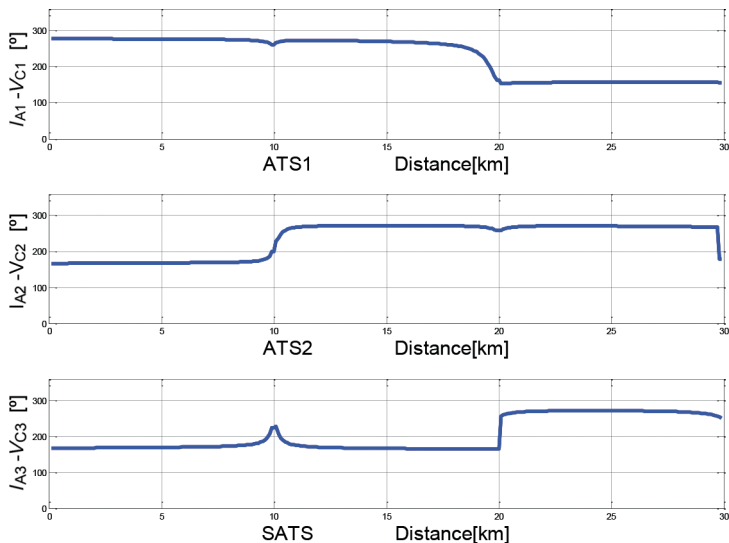


Figure 13: Phase angles between I_A and V_C at different ATS. Fault between feeder and rail. Two trains are placed at subsections A and C.

4 CONCLUSIONS

The influence of the high-speed trains consumption has been studied in the operation of a novel ground fault location method.

For this purpose a computer simulation model has been developed. Numerous simulations have been performed including one and two trains in the same section doing short circuits in the catenary and feeder along the 30 km of the section.

Although the power consumed by the high-speed trains slightly modify the theoretical 90° phase shift in case of ground fault, according to the results of all the simulations performed, the operation of the new ground fault identification method is correct, as long as the characteristic angle setting (previously set to $\pm 30^\circ$) of the directional overcurrent protection relay is properly modified [11]. The new value of the setting depends on the electrical section to be protected.

REFERENCES

- [1] Pilo, E., Rouco, R. & Fernandez, A., A reduced representation of 2×25 kV electrical systems for high-speed railways. *Proceedings of the 2003 IEEE/ASME Joint Rail Conference*. Chicago, IL, pp. 199–205, 2003.
- [2] Courtois, C., Why the 2×25 kV alternative? [autotransformer traction supply]. *50 kV Autotransformer Traction Supply Systems – The French Experience, IEE Colloquium*, pp. 1/1–1/4, 1993.
- [3] Han, Z., Zhang, Y., Liu, S. & Gao, S., Modeling and simulation for traction power supply system of high-speed railway. *Power and Energy Engineering Conference (APPEEC)*, Wuhan, China, pp. 1–4, 2011.
- [4] Richards, S.H., Application benefits of modern microprocessor distance protection for AC electrified railways. *Sixth International Conference on Developments in Power System Protection (Conf. Publ. No. 434)*: Nottingham, UK, pp. 338–341, 1997.
- [5] Zhou, Y., Xu, G. & Chen, Y., Fault location in power electrical traction line system. *Energies*, **5**, pp. 5002–5018, 2012. DOI: [10.3390/en5125002](https://doi.org/10.3390/en5125002)
- [6] AREVA T&D, *Network Protection & Automation Guide*, Alstom Grid: UK, pp. 354–363, 2002.
- [7] Han, Z., Liu, S., Gao, S. & Bo, Z., Protection scheme for China high-speed railway. *10th IET International Conference on Developments in Power System Protection (DPSP 2010), Managing the Change*, Manchester, pp. 1–5, 2010.
- [8] Millard, A., Taylor, I.A. & Weller, G.C., AC electrified railways-protection and distance to fault measurement. *Proceedings of the 1995 International Conference on Electric Railways in a United Europe*, Amsterdam, pp. 73–77, 1995.
- [9] Wang, C. & Yin, X., Comprehensive revisions on fault-location algorithm suitable for dedicated passenger line of high-speed electrified railway. *IEEE Transactions on Power Delivery*, **27(4)**, pp. 2415–2417, 2012. DOI: [10.1109/TPWRD.2012.2207270](https://doi.org/10.1109/TPWRD.2012.2207270)
- [10] Xu, G., Zhou, Y. & Chen, Y., Model-based fault location with frequency domain for power traction system. *Energies*, **6**, pp. 3097–3114, 2013. DOI: [10.3390/en6073097](https://doi.org/10.3390/en6073097)
- [11] Serrano, J., Platero, C.A., López-Toledo, M. & Granizo, R., A novel ground fault identification method for 2×25 kV railway power supply systems. *Energies*, **8(7)**, pp. 7020–7039, 2015. DOI: [10.3390/en81010993](https://doi.org/10.3390/en81010993)